Chapter 16. Gamma-t Jump System

16.1. System Description and Lattice Layout

W. Chou

In the present Main Injector, the injection energy is 8 GeV and maximum energy 120 or 150 GeV (depending on the operation mode). Transition crossing is at $\gamma_t = 21.6$. In the MI baseline design, no γ_t-jump system was included. However, when the beam intensity is increased by a factor of five, as assumed in PD2, simulation shows that emittance dilution and beam loss will occur (see Section 14.2). Furthermore, from experience at other machines (e.g., the AGS at BNL, the CERN PS and the KEK PS), transition crossing could become a severe bottleneck in high intensity operation. Therefore, a γ_t-jump system is necessary when we plan to upgrade the MI beam intensity.

The conceptual design of a γ_t-jump system for the Main Injector was completed in 1997 and reported in Ref. [1]. It is a so-called first-order system employing local dispersion inserts at dispersion-free straight sections. The design goal is set as follows. The normal ramp rate of the MI is about 240 GeV/s. In order to have an effective γ_t-jump, the jump rate should be at least an order of magnitude higher. Thus the system was chosen to provide a $\Delta\gamma_t$ from +1 to -1 within 0.5 ms. This gives a jump rate of 4000 s^{-1}, about 17 times faster than the normal ramp rate.

The system consists of 8 sets of pulsed quadrupole triplets. Each triplet has two quads in the arc and one of twice integrated strength in the straight section, with a phase advance of π between each quadrupole. The perturbation to the original lattice is localized. In particular, the dispersion increase during the jump is small ($\Delta D_{max} \approx 1$ m), which is the main advantage of a first-order jump system. Each triplet is optically independent from the others and provides roughly 1/8 of the total required jump amplitude (i.e., $\Delta\gamma_t \approx 0.25$ per triplet). The power supply uses a GTO as the fast switch and a resonant circuit with a 1 kHz resonant frequency. The beam pipe is elliptical and made of Inconel 718. It has low electrical conductivity σ and high mechanical strength so eddy current effects are relatively small. (The eddy current effects scale as σd, where d is the pipe wall thickness. The σd value of Inconel 718 is about four times lower than that of stainless steel.)

An alternative to a γ_t-jump system is the focus-free scheme using a higher harmonic rf cavity. Although this scheme is believed to be good for tackling nonlinear effects during transition crossing, its effectiveness is unknown for curing collective effects (e.g., bunch length mismatch due to space charge, negative mass instability after transition). Therefore, it will not be discussed in this chapter.

The locations of the required 24 pulsed quadrupoles (PQ) are listed in Table 16.1 and shown in Fig. 16.1. Each triplet consists of three quads, marked as PQxxx, in which xxx is the nearest main quad number of the Main Injector. In Table 16.1, eight locations are marked with "ok," meaning that there is no conflict with the existing components in the

ring. At fifteen of the locations notes indicate measures needed in order to fit the pulsed quadrupoles into the ring. However, one location (PQ322) in MI-32 may have to be excluded because of the antiproton beam transport line from the Recycler (which did not exist when the design was carried out in 1997). There are two possible solutions to this problem. One is to use 7 triplets instead of 8. This would lead to a reduction of 1/8 in jump amplitude, which is acceptable. Another is to find a new location for this triplet, which is yet to be studied.

Table 16.1. γ_t-Jump System Pulsed Quadrupole Locations

PQ104 – relocate a multiwire monitor
PQ108 – remove a sextupole
PQ112 – ok

PQ226 – shorten BPM by 1-inch or eliminate the bellows
PQ230 – same as PQ226
PQ302 – relocate a Schottky detector

PQ322 – interference with the MI-32 antiproton line from the Recycler
PQ326 – same as PQ108
PQ330 – ok

PQ334 – ok
PQ338 – ok
PQ400 – move the abort kicker downstream by 1 m

PQ404 – ok
PQ408 – same as PQ108
PQ412 – ok

PQ526 – same as PQ226, plus relocate an LLRF pickup
PQ530 – same as PQ526
PQ602 – relocate the Desert Air box

PQ622 – move the antiproton extraction kicker by 1 m
PQ626 – same as PQ108
PQ630 – remove a trim quad

PQ634 – ok
PQ638 – ok
PQ100 – move the γ_t quad downstream by 40-inches to avoid SQA852

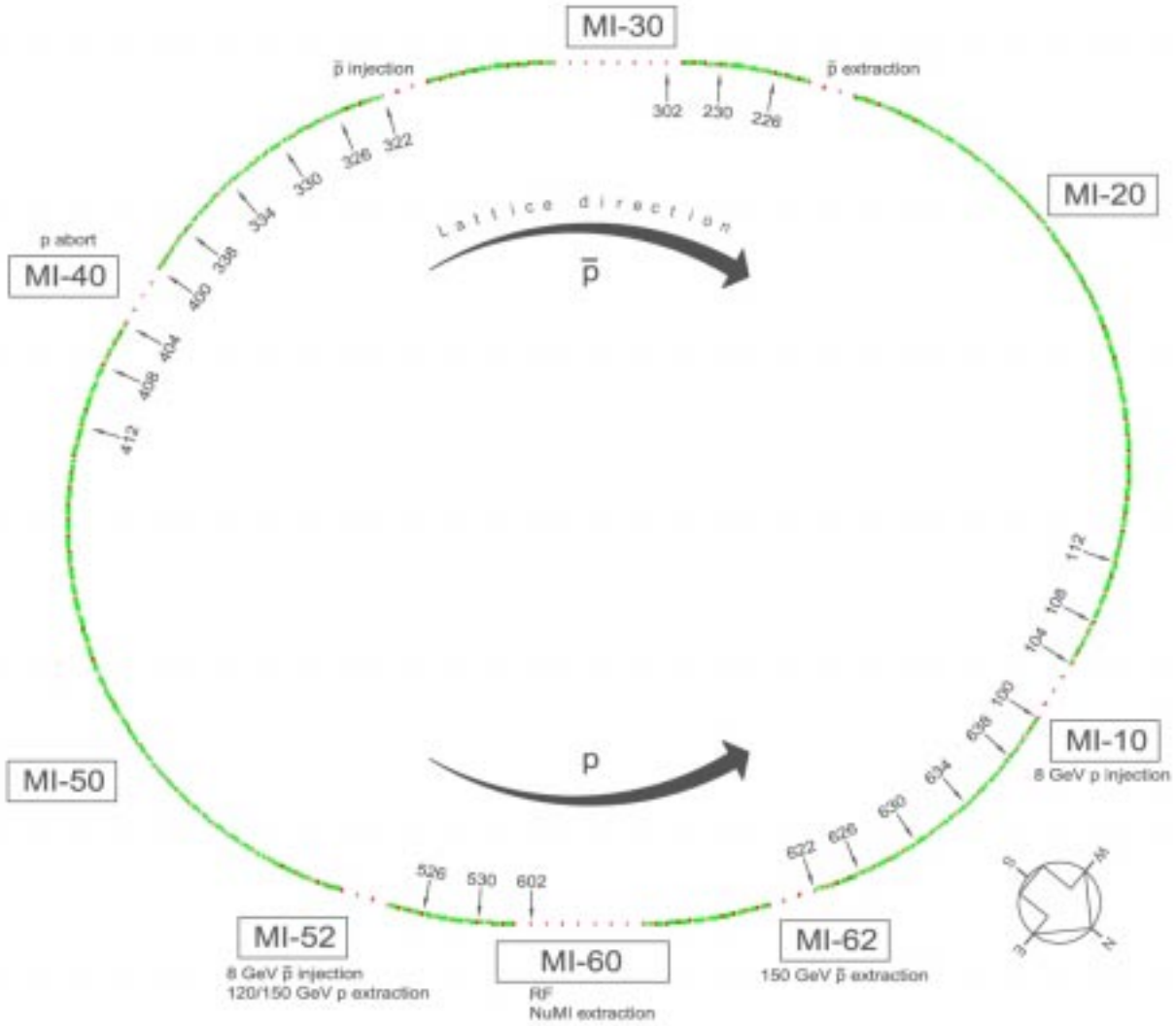

Figure 16.1. Gamma-t jump system lattice layout - Locations of the 24 pulsed quads in the Main Injector. (Red indicates the MI main quadrupoles, green the main dipoles.)

16.2. Pulsed Quadrupoles

I. Terechkine

16.2.1. Introduction

This section describes the pulsed quadrupole design for the Main Injector gamma-t jump system. Preliminary design criteria were described by B. Brown [2] and W. Chou [1] and provide a starting point for this section. Attention is paid to power losses in the quadrupole core, coil and vacuum pipe, because these losses will influence the power supply design and performance. The main feature of the quadrupole is its operational frequency requirement. The maximum frequency in the current pulse spectrum is about 1 kHz. The bipolar current pulse consists of three parts: a relatively slow current rise (about 3 ms) until maximum current is achieved, a fast current drop (0.5 ms) with current polarity reverse, and then a slow current decay (3 ms). The current pulse is to be applied to the quadrupole only once during the acceleration cycle, so heating is not so important. Nevertheless, eddy currents induced in the steel core (if the core is made from steel laminations), copper wire and stainless steel vacuum pipe can change significantly the current pulse parameters. That's why it is necessary to analyze the effect of these eddy currents on the magnet equivalent circuit parameters. Relevant system requirements are listed in Table 16.2.

Table 16.2. Pulsed Quadrupole System Parameters

Required integrated gradient (T)	0.85
Vacuum pipe cross-section (elliptical) (inch.)	2.4×1.125
Field quality within 1 inch radius circle	2%
Maximum quadrupole length (inches)	17
Maximum current (A)	200
Maximum voltage (V)	ALAP

16.2.2. Magnetic design

It is desired to keep the voltage as low as possible (ALAP). This necessitates reducing the total volume of magnetic field. It is possible to achieve the required field quality using an unsymmetrical pole design and simple flat coil fitted around the vacuum pipe. Figure 16.2 shows one quarter of a quadrupole cross-section, and Table 16.3 gives core cross-section base point coordinates.

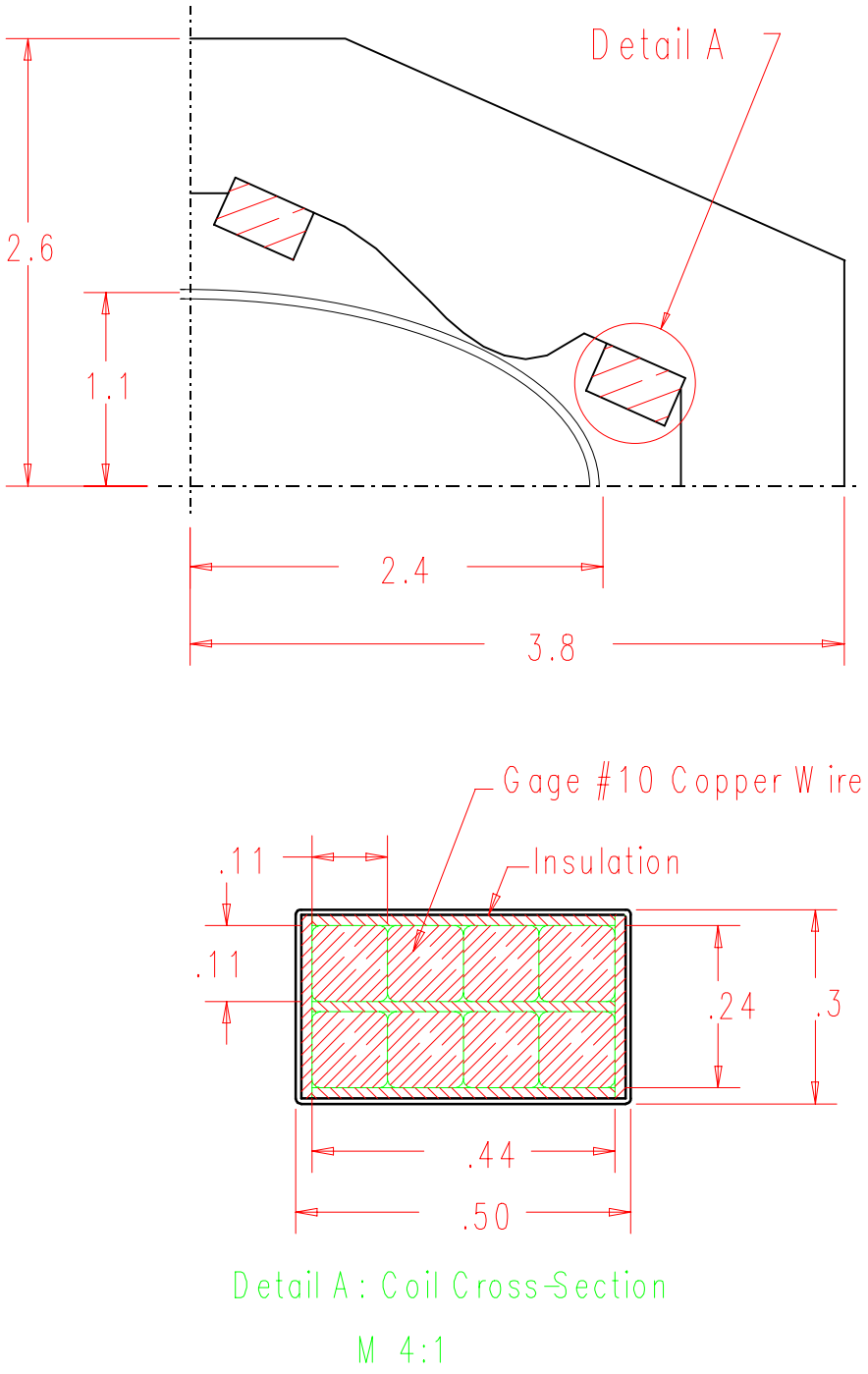

Figure 16.2. Pulsed Quadrupole Cross-Section Layout

Because the coil in this design plays a rather significant role in shaping the field, it should be epoxy impregnated to provide necessary rigidity and reproducibility of cross-section dimensions. Coil positioning tolerances are about ±0.010 inches, not a big problem for this kind of coil.

Table 16.3. Core Cross-Section Base Points Coordinates

X (in)	Y (in)	X (in)	Y (in)	X (in)	Y (in)	X (in)	Y (in)	X (in)	Y (in)
0.0	1.7	1.08	1.38	1.825	0.76	2.879	0.626	0.9	2.7
0.222	1.7	1.394	1.07	1.95	0.735	2.85	0.561	0.0	2.7
1.263	0.791	1.491	0.97	2.075	0.76	2.85	0.0	0.0	1.7
0.719	1.588	1.587	0.89	2.29	0.888	3.80	0.0		
0.9	1.508	1.706	0.81	2.422	0.829	3.8	1.3		

With total Ampere-turns in the coil Iw = 1623.8 A (corresponding to 20,000 A/in^2 of coil average current density), the gradient G = 560 Gauss/in; so about 15.2 inches of a core length is required to meet the integrated strength requirement. Figures 16.3 and 16.4 show the field distribution, and Figure 16.5 shows field quality for horizontal and vertical axes.

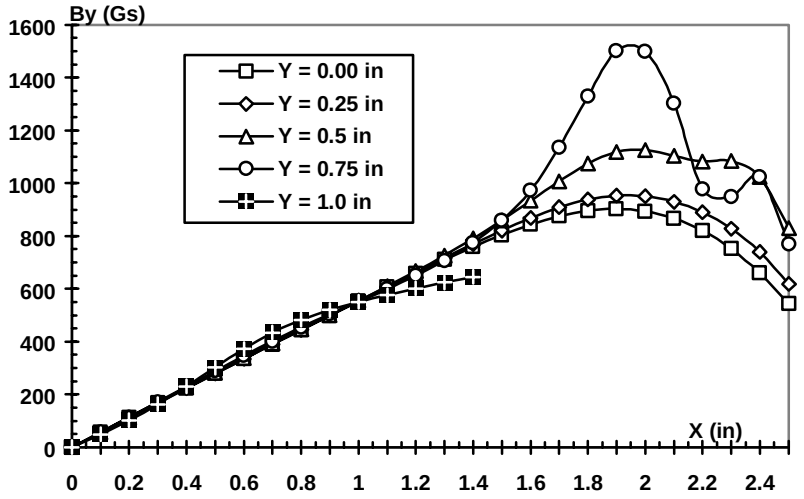

Figure 16.3. Vertical magnetic field distribution in the quadrupole cross-section.

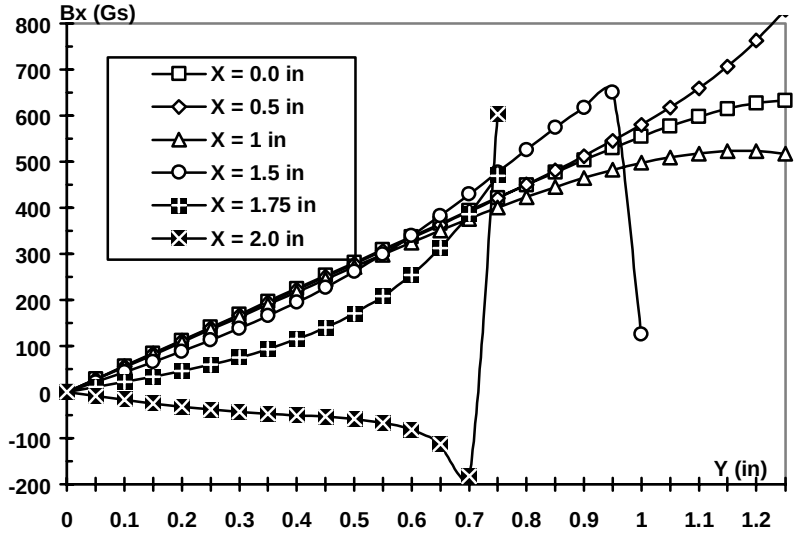

Figure 16.4. Horizontal magnetic field distribution in the quadrupole cross-section.

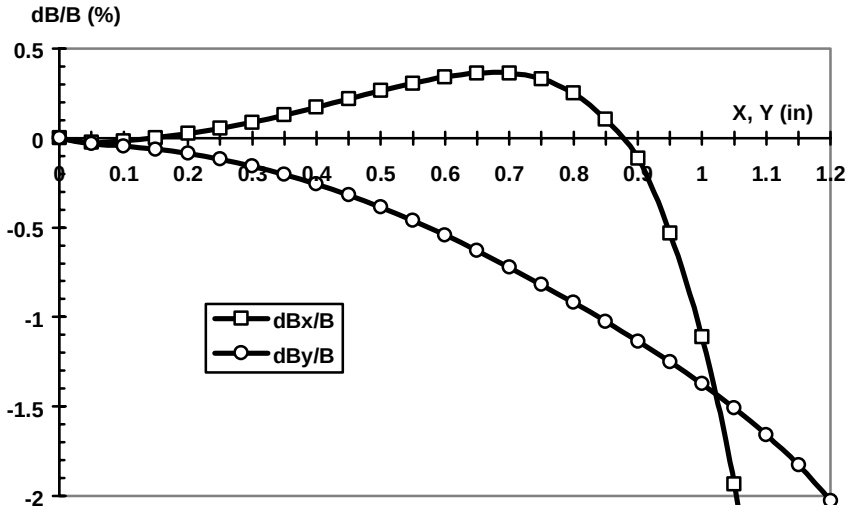

Figure 16.5. Quadrupole field quality

The magnetic flux for one pole at nominal gradient is 2530 G-in^2 per 1 inch of the magnet length, or 0.0025 Tm^2 for the 15.2 inch length quadrupole. Table 16.4 contains data used to choose coil parameters based on the required integrated strength.

Table 16.4. Quadrupole Parameters

Number of turns per pole	6	8	10
Inductance (μH)	225	400	620
Current (A)	270	200	160
Voltage (V)	375	500	630
Resistance (mOhm)	12	20	32

To choose coil wire gauge, it is useful to calculate the copper skin layer thickness. This is about 0.09 inch, so the wire thickness cannot be significantly larger than 0.18 inch. Fig. 16.2 and Table 16.4 use #10 square copper wire, which has thickness about 0.1 inches.

16.2.3. Eddy Current Losses

To form the required current pulse, the power supply described in [2] made use of LCR resonant circuits. The quality factor of this circuit is affected not only by the coil wire resistance, but also by power losses due to eddy currents induced in the vacuum pipe, in the steel core, and in the coil itself. To compare power losses due to eddy currents in different magnet parts, it is convenient to describe these losses in terms of an equivalent parallel resistance R. Then wire losses caused by the excitation current can be described by an equivalent parallel resistance R_{wire} that can be found if we know the wire series resistance r_{wire} (Table 16.4):

$$R_{wire} = \omega^2 L^2 / r_{wire}$$

This formula gives R_{wire} = 315 Ohm at 1000 Hz for an 8-wire pole coil. (L is the total magnet inductance). For comparison, the magnet impedance ωL = 2.5 Ohm.

16.2.3.1. Vacuum pipe power losses

In order to find vacuum pipe losses, it is necessary to know the current density distribution in the pipe wall. To calculate the current density distribution, the normal magnetic field distribution was found along the pipe circumference using the OPERA-2D magnetic modeling program. Figure 16.6 shows the normal magnetic field distribution for a vacuum pipe made of flat surfaces that approximate an elliptical cross-section. In this picture, s is the distance along the pipe wall beginning from the point (0, 1.1) counterclockwise to the point (2.4, 0) (see also Fig. 16.2). The field distribution is shown only for one quarter of the cross-section.

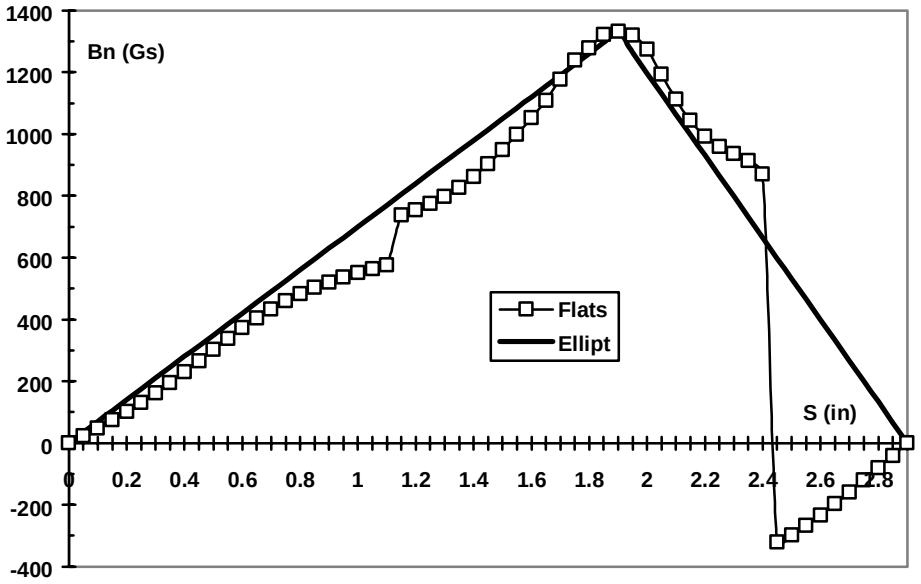

Figure 16.6. Normal magnetic field distribution along the vacuum pipe

To simplify the problem a linear normal field distribution was used along the pipe cross-section border:

B_n (G) = 700 s if s < 1.9 inches,
B_n (G) = 3857 - 1330 s if s > 1.9 inches.

This distribution is the solid line in Fig. 16.6. Converting inches to meters and Gauss to Tesla gives:

B_n (T) = 2.756 s (m) if 0 < s < s1,
B_n (T) = 0.3857 - 5.236 s (m) if s1 < s < s2.

In this expression s1 = 0.04826 m is the point with the maximum magnetic field B_m, and s2 = 0.07366 m is a quarter of the vacuum pipe perimeter. Using the simple expressions for the normal magnetic field distribution above and applying the condition that the total current in the pipe is zero, we find the pipe wall current distribution:

$$j(s) = 1/6 \cdot \omega \cdot B/\rho \cdot (2 \cdot s2 - s1 - 3 \cdot s^2/s1) \qquad \text{if } s < s1,$$
$$j(s) = 1/6 \cdot \omega \cdot B/\rho \cdot (3 \cdot s^2 - 6 \cdot s \cdot s2 + s1^2 + 2 \cdot s2^2)/(s2 - s1) \qquad \text{if } s > s1.$$

This distribution is shown in the Fig. 16.7.

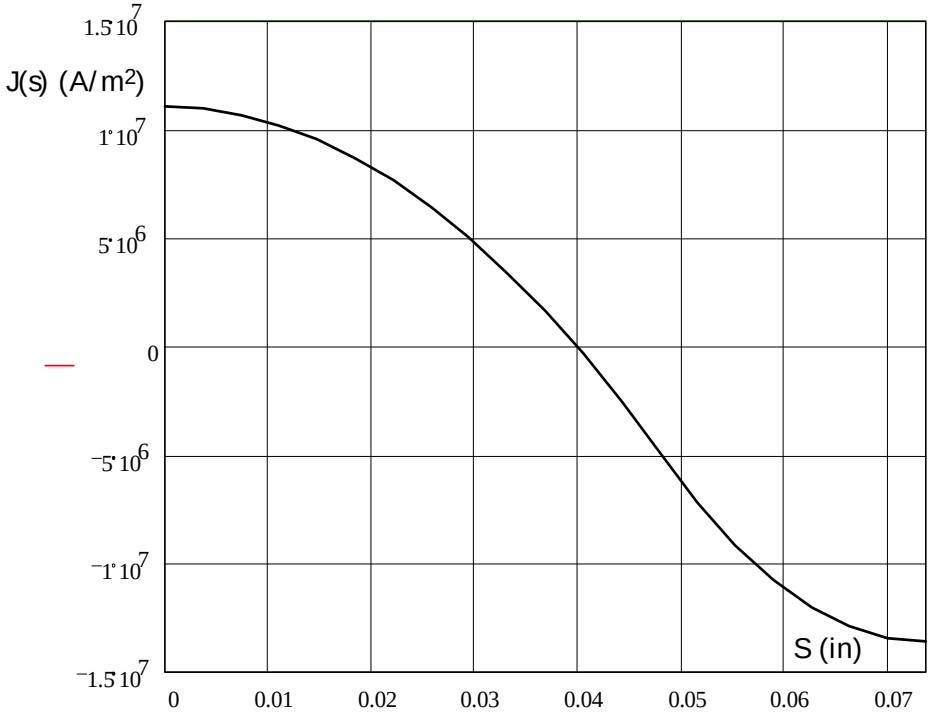

Figure 16.7. Current density distribution in the vacuum pipe wall

Now it is easy to find total power in the pipe wall:

$$P = l \cdot t \cdot \rho \cdot \oint_p j^2 ds \ ,$$

where l is the magnet length and t the wall thickness. Integrating over the vacuum pipe perimeter gives for a 25-mil wall Inconel 718 pipe ($\rho = 1.25 \times 10^{-6}$ Ohm·m) the maximum instantaneous power:

$$P \approx 7{,}300 \text{ W}$$

The parallel resistance that corresponds to this power loss $R_{pipe} = U^2/P \approx 34$ Ohm. Comparing this loss resistance value to the quadrupole intrinsic impedance (2.5 Ohm) gives the circuit quality factor $Q \approx 13.5$.

16.2.3.2 Core power losses

If the magnet core is assembled from steel laminations, two factors cause power losses: steel eddy currents and hysteresis. Because hysteresis losses scale proportionally to the operation frequency, and eddy current losses grow as the square of the frequency, we can expect at 1000 Hz eddy current losses will dominate.

Two different parts of the magnetic flux generate the steel eddy currents. The first is the main flux that goes along the laminations; the second is the end flux that is perpendicular to the lamination surface.

Main flux

Eddy current maximum instantaneous power losses in a laminated core can be estimated using the expression:

$$P_{st} = 1/12 \cdot \omega^2 \cdot B^2 \, t^2/\rho \cdot V,$$

where V is steel volume and B stands for steel magnetic field. With B = 0.14 T, the average steel magnetic field from magnetic calculations, and choosing M-15 silicon steel ($\rho = 5 \times 10^{-7}$ Ohm·m) with lamination thickness t = 0.014 inch (0.355 mm), we have P_{st} = 120 W. Parallel resistance that accounts for this loss component is R_{st} = 2100 Ohm. Because the main flux loss resistance is rather high, we can use a thicker lamination. But this would reduce the steel effective stacking factor because flux is not distributed equally through the cross-section. Skin layer thickness for the silicon steel at 1000 Hz can be calculated as

$$\delta^{-1} = (\omega\mu\mu_0/2\rho)^{1/2}$$

Using $\mu = 5000$, a typical value for silicon steel at low field level, we have $\delta = 0.15$ mm; so a lamination thickness t = 0.3 mm is close to optimal.

End flux

Because it is practically impossible to make a coil that exactly follows the magnet pole edge (current density limitations), part of the magnetic flux goes perpendicular to the magnet end plane. Eddy currents induced in laminations result in a limitation on axial flux penetration thickness, but this thickness is not equal to the thickness of the skin layer. Magnetic modeling shows that if the coil is located near the pole end, it is possible to calculate the depth of axial field penetration using a linear magnetic field drop along the coil thickness d:

$$j \approx H_m(1/c-1/d),$$

or $$j \approx B_m/\mu\mu_0(1/c-1/d).$$

Permeability μ should be taken close to 1 because most of the magnetic field circulation circuit passes through air, and only part of it goes inside the core. On the other hand, current density

$$j = U/(\rho \cdot p),$$

where $U = \omega \cdot F$ is voltage generated by changing flux F through the pole surface S, and p is the pole perimeter. To calculate end flux, we approximate the pole as a trapezoid with small side $w_0 = 0.5$ inches, base side $w_1 = 2$ inches, and height equal to the coil thickness (see Fig. 16.2). Then the total flux F through the pole is:

$$F = \int B_m(1-y/d)(w_0+3 \cdot w_0 \cdot y/d)dy,$$

where integration is performed along the pole height (0 to d). Calculation gives $F = 1.3 \times 10^{-5}$ Tm^2, about 0.5% of the total magnet flux. Combining these equations, we have a simple estimate for the equivalent eddy current penetration depth c:

$$c^{-1} = 1/d + \omega \cdot \mu_0 \, F/(B_m \cdot p \cdot \rho)$$

Because the flux F can be written as $F = k^{-1} S B_m$, where k is a coefficient depending on details of coil positioning and pole shape, we can rewrite the above equation as

$$c^{-1} = d^{-1} + \omega \cdot \mu_0/(k \cdot \rho) \cdot S/p$$

For our specific coil-pole case, we have $S = 0.375$ in^2, $p = 2$ in, and $k = 2.56$. Substituting into the above equation we have $c = 6.25$ mm (0.25 inches).

On the other hand, the end flux is taken from the nearest lamination layers. The total thickness of this layer is approximately equal to half of the magnet gap, about 1 inch for this quadrupole. The effect of eddy currents on field distribution is a reduction of axial field near the pole and an increase of the gap field near the magnet end.

Comparing the two numbers for border layer thickness: 0.25 inches and 1 inch, we conclude that in the case of our magnet eddy currents change the steady state end magnetic field distribution. Taking this into the account, and providing an additional margin by choosing the maximum number for end flux penetration depth, the distribution of the axial magnetic field near the magnet end can be written as:

$$B_z(y,z) = B_m(1-y/d)(1-z/c),$$

where $c = 1$ inch.

When we know the normal magnetic field distribution, we can calculate the induced current density in the pole. To simplify the problem, we use a rectangular pole shape with width w and the same end surface area. This gives more power than with the real pole because a larger volume is carrying a larger current density. We also assume that only the x current component is present and that the steel resistivity is zero in the region where the magnetic field is zero (beyond the pole tip). Then the current density can be found by solving a system of field equations and boundary conditions:

$$\text{rot } E = -\, dB_z/dt,$$
$$j = E/\rho,$$
$$E = E_x,$$
$$j_x = 0 \quad \text{if } y \geq d.$$

The solution gives the current density:

$$j_x = \omega B_m d/2\rho \cdot (1-z/c) \cdot (1-(y/d)^2).$$

Power losses can be found easily if we know the current density distribution:

$$P_{end} = \frac{\omega^2 \, B_m{}^2 d^2 w}{2\rho} \cdot \int_0^c dz \cdot (1-\frac{z}{c})^2 \cdot \int_0^d dy \cdot (1-\frac{y^2}{d^2})^2$$

After integration we have finally:

$$P_{end} = 0.04 \cdot \rho^{-1} \cdot d^3 \cdot c \cdot w \cdot \omega^2 \cdot B_m{}^2$$

Power loss per pole is about 25 W and total power losses per magnet

$$P_{tot} \approx 200 \text{ W}$$

The effective equivalent resistance for end losses is $R_{end} \approx 1250$ Ohm.

16.2.3.3 Coil eddy current losses

Because coil turns are located in the space between the quadrupole poles, the pole flux partially penetrates into the coil volume and induces an eddy current that is an additional source of power losses. To make an estimate of these losses we assume that the flux enters perpendicular to the coil wire surface. We can write down the expression:

$$dP_{Cu} = 1/12 \cdot \rho_{Cu}{}^{-1} \, \omega^2 \cdot B_w{}^2 \, t^2 \cdot dV_w ,$$

where B_w is the magnetic field that penetrates the wire. Applying Ampere's law to find B_w along the coil surface and integrating over all quadrupole coil wires, we have:

$$P_{Cu} \approx 1/36 \cdot \omega^2 \cdot (Iw)^2 \, \mu_0{}^2/\rho_{Cu} * t^4 \cdot l_w/h_w{}^2$$

where t is square copper wire thickness, Iw is the coil Ampere-turns, h_w stands for maximum distance from coil wires to the quadrupole plane of symmetry, and l_w is total wire length. With Iw = 1630 A and l_w = 35 m for #10 square copper wire (t = 0.1 inches), we have $P_{Cu} \approx 760$ W and $R_{Cu} = 330$ Ohm.

Taking all the above into the account, we may represent the magnet as an equivalent circuit. It consists of an inductance with impedance ωL. It is connected in parallel to several resistive elements with resistance values shown in the Table 16.5.

Table 16.5. Parameters of the Magnet Equivalent Circuit

Element	Inductance	Wire Resistance	Vacuum Pipe	Core Lamination	Core Ends	Wire Eddy
Symbol	ωL	R_w	R_p	R_c	R_e	R_{Cu}
Impedance	2.5	315	34	2100	1250	330

Clearly the main power loss is due to eddy current losses in the vacuum pipe. Nevertheless, the quality factor of circuit is about 13.5 and allows use of a resonant pulse-forming circuit.

16.2.4. Conclusion

The design of a pulsed quadrupole for the MI gamma-t jump system is feasible. Field quality can be maintained within required limits, the core shape can be optimized to reduce significantly end eddy current losses, and the coil can be designed to meet current requirements. If four quadrupoles are connected in series, about 5000 V of test voltage is required to insure adequate magnet insulation. This requirement can be significantly weaker if bi-polar power supply is considered. Wire resistance losses and core and coil eddy current losses are low enough to allow magnet operation in a resonant circuit. The major part of power losses occur in the Inconel-718 vacuum pipe, but even these losses allow use of a pulse-forming circuit as suggested in [2].

16.3. Power Supplies

D. Wolff

The MI gamma-t jump power supply system consists of 8 power supplies. Each power supply drives a four-magnet quadrupole string. The power supply design is shown in Figure 16.8.

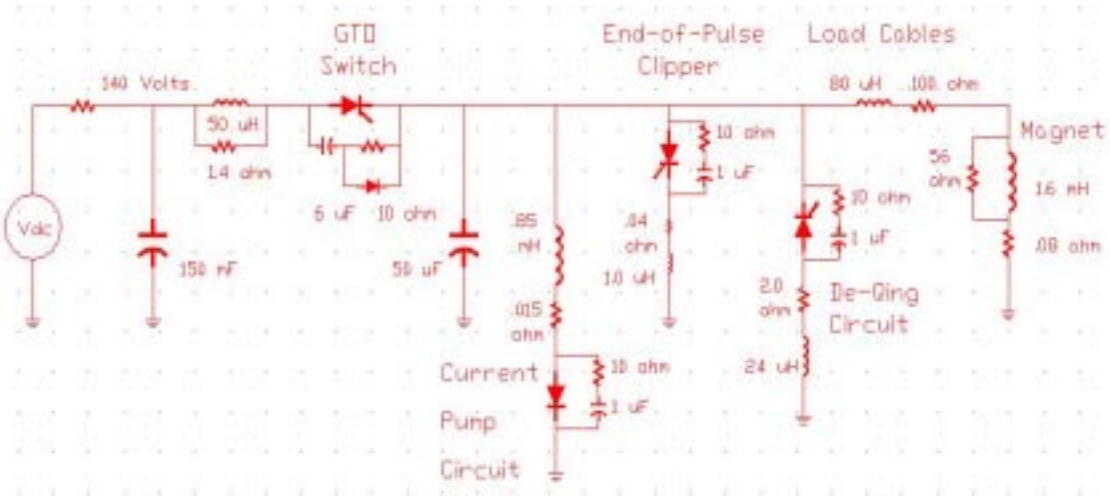

Figure 16.8. Circuit diagram of the MI gamma-t jump power supply system.

Figure 16.9 shows the various magnet current waveforms that can be produced by the power supply:

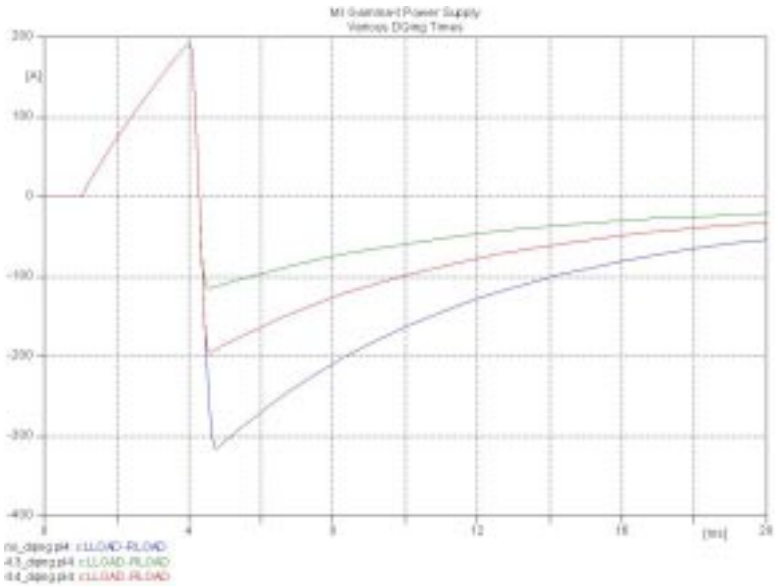

Figure 16.9. The magnet current waveforms for various De-Qing times.

A short description of circuit operation follows. The pulse begins when the GTO (gate turn-off thyristor) is turned ON. This applies 140 volts to the load and charges the load current to 195 amps in 3 ms. At this time the GTO is turned OFF and the magnet load acting as a resonant circuit with the 50 μF capacitor rings through one half cycle.

Turning ON the End-of-Pulse clipper SCR allows the magnet current to return to zero following the L/R time constant of the load and load cables. To control the peak negative current, the De-Qing circuit SCR can be turned ON before the pulse reaches its maximum negative value. The current will then return to zero as mentioned above. The waveforms in Figure 16.3.2 show two such De-Qing events at –200 amps and –120 amps. The current pump circuit is charged while the GTO is ON. When the GTO is turned OFF the current in the pump circuit adds to the negative load current thereby producing the maximum desired negative current.

16.4. Beam Pipes

A. Chen

The beam pipe of the MI gamma-t jump system will be made of thin metallic vacuum tight beam tubes. [4] Inconel 718 is chosen because it has excellent mechanical strength and high electrical resistance so that it can minimize the eddy current effects within a pulsed magnetic field. It can also be machined and welded without special cares. The parameters are listed in the following table 16.6:

Table 16.6. MI Gamma-t Jump System Beam Pipe Parameters

Material of Tube	Inconel 718, 0.025” Sheet
Material of End Flange	Inconel 718, 3/16” Sheet
Lengths of Tube	0.5 m (16 sections), 1.0 m (8 sections)
Major Diameter	4.89 inches
Minor Diameter	2.09 inches
Material of transition flanges	S.S. 316

The thin Inconel sheet will be cut into proper size, and then be rolled into round tube followed by electron beam welding. The round tubes will then be pressed to achieve an elliptical shape and heat-treated to increase mechanical strength. The tubes will then be welded to Inconel 718 flanges. These flanges and the stainless steel transition flanges are formed into a single piece.

16.5. Controls

M. Shea

The gamma-t jump system planned for PD2 consists of eight sets of magnets with their associated pulsed power supplies spaced around the Main Injector. This system would require an IRM at each of the eight locations to provide the analog control, timing triggers and data acquisition needed to operate the power supplies and to return readings to the Accelerator Network (ACNET) consoles. Timing requirements do not appear to be stringent and should be satisfied by the Tevatron-clock-based delay timers normally supplied by a Linac-style Front End computer. Analog control, slow analog readings of

power supply parameters and snapshot readings of power supply waveforms will be provided by an IRM at each of the eight locations.

References

[1] W. Chou, et al. "Design of a Gamma-t Jump System for Fermilab Main Injector," PAC 1997 Proceedings, pp. 994-996.

[2] B. Brown, Beams Division, Fermilab, private communication.

[3] T. J. Gardner, private communication.

[4] J.R. Leibfritz, "FNAL Main Injector Gamma-t Jump System Beamtube Design," PAC 1997 Proceedings, p. 3601.